Korean J. Chem. Eng., 33(9), 2738-2746 (2016)
DOI: 10.1007/s11814-016-0146-y

pISSN: 0256-1115
eISSN: 1975-7220

Physical characteristics and *in vitro* skin permeation of elastic liposomes loaded with caffeic acid-hydroxypropyl-β-cyclodextrin

Na Ri Im, Kyoung Mi Kim, Suh Ji Young, and Soo Nam Park†

Department of Fine Chemistry, Cosmetic R&D Center, College of Energy and Biotechnology,
Seoul National University of Science and Technology, 232, Gongneung-ro, Nowon-gu, Seoul 01811, Korea
(*Received 7 April 2016 • accepted 30 May 2016*)

Abstract−We developed a drug-in-cyclodextrin-in-elastic liposomes (DCEL) system to enhance transdermal delivery of caffeic acid (CA). Hydroxypropyl-β-cyclodextrin (HP-β-CD) was used as a hydrophilic CD. Elastic liposomes (EL) contained polyethylene glycol-free Tego® care 450 as an edge activator. Properties of the CA-HP-β-CD inclusion complex loaded in EL (CD-EL) as DCEL system were compared to characteristics of conventional liposomes (CL), EL, and CD-CL. Particle size, deformability, entrapment efficiency (EE%), stability, and vesicle morphology were characterized in liposome preparations. In addition, *in vitro* release and skin permeation were analyzed. We found that including Tego® care 450 reduced vesicle size and increased membrane deformability. The addition of HP-β-CD enhanced CA EE% of liposomes almost 1.6-fold that of liposomes without HP-β-CD. Moreover, CD-EL complex showed better controlled release profiles and higher skin permeability than CL and EL. We propose that the DCEL system can be a promising drug delivery vehicle for transdermal delivery of CA.

Keywords: Caffeic Acid, Hydroxypropyl-β-cyclodextrin, Elastic Liposome, Drug-in-cyclodextrin-in-elastic Liposome, Skin Permeation

INTRODUCTION

Stratum corneum (SC), the outermost layer of the skin, serves as a protective barrier to potentially harmful environmental agents. However, it simultaneously acts as a penetration barrier by blocking the delivery of pharmacologically active compounds via the transdermal route [1]. Therefore, transdermal drug delivery systems (TDDS) have been developed to make this barrier more permeable and to enhance transdermal delivery of various bioactive substances [2]. Liposomes are spherical vesicles composed of phospholipid bilayers similar to the cell membrane. Due to their biocompatibility, biodegradability, and low toxicity, liposomes are frequently used in cosmetic and pharmaceutical preparations as TDDS [3]. However, conventional liposomes (CL) are not efficient carrier systems for transdermal drug delivery because they do not penetrate deeply into the skin, but rather remain confined to the upper SC layer [4]. Thus, novel elastic vesicles have been developed to complement the low skin penetration ability of CL [5].

Elastic liposomes (EL), which were first introduced in 1992 by Cevc and Blume [5], typically consist of phospholipids and an edge activator. The edge activator is often a single chain surfactant with a high radius of curvature that destabilizes lipid bilayers of the vesicles and increases deformability of the bilayers. Due to these structural features, EL provides easier penetration through SC and more efficient delivery of bioactive compounds into the skin compared to possibilities offered by CL [6]. Polyethylene glycol (PEG) is a non-toxic and water-soluble polymer widely used in cosmetic formulations as a surfactant and humectant. However, it has been reported that PEG may be a source of impurities, such as 1,4-dioxane and ethylene, in cosmetic manufacturing processes. PEG can also cause systemic toxicity and skin sensitization [7]. For this reason, the use of PEG-free surfactants has been steadily increasing recently. For example, elastic liposomes with Tego® care 450 (polyglyceryl-3 methylglucose distearate) as a PEG-free surfactant have been described in previous reports [8,9].

Liposome can encapsulate both hydrophilic and hydrophobic drugs into the internal core and lipid membranes of liposomes, respectively [3]. However, the entrapment of some hydrophobic drugs in the lipid bilayer can be problematic as drugs decrease liposome stability by destabilizing the structural integrity of bilayers. Moreover, drugs incorporated in the membrane bilayer, rather than in the aqueous liposome core, are prone to a more rapid release [10]. Several researchers have proposed dissolving hydrophobic drugs in an ethanol [11], conjugating the surface with PEG, or complexation with cyclodextrin [12] to circumvent these problems. Entrapment of water-soluble drug-cyclodextrin (CD) inclusion complexes in the aqueous core of liposomes, i.e., construction of a drug-in-CD-in-liposome (DCL) system, was proposed as an interesting strategy in 1994 [13]. Recently, drug-in-cyclodextrin-in-elastic liposomes (DCEL), a new delivery system for cutaneous administration, which combined the advantages of drug-CD inclusion complexes and those of elastic liposomes, was described by Jain et al. [14]. The DCEL system increased drug solubility and permeation through the skin, thus enhancing drug bioavailability via the transdermal route [15]. CDs are cyclic (β-1,4)-linked oligosaccharides of D-glucopyranose containing a relatively hydrophobic central cavity and a

†To whom correspondence should be addressed.
E-mail: snpark@seoultech.ac.kr

hydrophilic outer surface. Complexation of drugs with CD increases drug solubility, improves its stability, and sustains drug release [16]. Hydroxypropyl-β-cyclodextrin (HP-β-CD), a hydrophilic derivative of β-CD, is the most frequently used CD for topical/transdermal delivery of drugs [17]. In addition, it has been used as a solubilizing agent and penetration enhancer in transdermal delivery [18].

Caffeic acid (3,4-dihydroxycinnamic acid, CA) is a well-known phenolic phytochemical found in fruit, vegetables, coffee beans, and *Glycyrrhiza glabra* root [19,20]. The pK_a of the carboxylic group of the CA is 4.44, while that of the phenolic groups of CA is 7.6 and 11.85. Thus, the carboxylic group should be completely ionized at pH 7.4 [21]. There have been many reports of the beneficial effects of CA, including antiviral, anti-inflammatory, antioxidant, and antidepressant activity. Furthermore, antimicrobial properties of CA against *Escherichia coli*, *Bacillus cereus*, *Staphylococcus aureus*, *Listeria monocytogenes*, and some yeast have been described. However, its poor aqueous solubility and low stability in presence of UV and oxygen complicates its utility for transdermal delivery [22,23]. These drawbacks can be partially overcome, as it has been reported previously that CA solubility can be increased by the use of water-soluble HP-β-CD inclusion complexes [24].

We prepared a DCEL system that combined the advantages of CD and EL to enhance skin permeation of CA. We examined several physico-chemical characteristics of our DCEL system, such as particle size, deformability, entrapment efficiency, stability, and vesicle morphology. In addition, *in vitro* release and skin permeation were evaluated. The objective of our study was to investigate the potential of this DCEL system for transdermal drug delivery.

MATERIAL AND METHODS

1. Material

L-α-phosphatidylcholine (from egg yolk, ≥60%; egg PC), cholesterol (≥99%), and caffeic acid were obtained from Sigma-Aldrich (St. Louis, MO, USA). Hydroxypropyl-β-cyclodextrin (MW 1541.54, HP-β-CD) was purchased from TCI (Tokyo, Japan). Tego® care 450 (polyglyceryl-3 methylglucose distearate) having HLB 11.5 was supplied by from Saimdang Cosmetics Co., Ltd. (Seoul, Korea). Solvents, such as 1,3-butylene glycol (1,3-BG), methanol, ethanol, chloroform, acetic acid, and acetonitrile, were of analytical grade.

2. Methods

2-1. Preparation of the CA-HP-β-CD Complex

The complex of CA and HP-β-CD was prepared by the freeze-drying method [25]. A previous study showed that the optimal stoichiometric molar CA : HP-β-CD ratio was 1 : 1 [24]. Therefore, to prepare the complex of CA and CD, 0.09 g (5 millimoles) CA and 0.77 g (5 millimoles) HP-β-CD were dissolved in 100 mL of distilled water. The solution was mixed by a magnetic stirrer at 300 rpm for 48 h. After that, the resulting solution was filtered through a 0.45-μm pore size filter (Minisart; CA, 26 mm) to remove the unencapsulated drug. The solution was frozen at −60 °C for 24 h and lyophilized in a freeze-dryer (Ilshin biobase, Seoul, Korea) for 48 h to obtain the complex powder. The amount of CA entrapped in the complex was determined by HPLC analysis.

2-2. Characterization of CA-HP-β-CD Complex

2-2-1. Scanning Electron Microscopy (SEM)

Morphological evaluation of CA, HP-β-CD, the CA-HP-β-CD inclusion complex, and a physical mixture of CA and HP-β-CD was performed by SEM (TESCAN VEGA3, Cranberry TWP, PA, USA). The dried samples were evenly distributed on SEM specimen stubs with double adhesive tape. Prior to examination, the samples were sputtered with gold, then the micrographs were obtained with an accelerating potential of 20 Kv under low vacuum.

2-2-2. X-ray Diffractometry (XRD)

The X-ray powder diffraction patterns were obtained with a D8 Advance XRD diffractometer (Bruker, Germany). The samples were irradiated with a Cu-K(α) radiation, at a voltage of 40 kV and a current of 40 mA. The scanning rate was employed for 2°/min over a diffraction angle of 2θ ranging from 5° to 90°.

2-3. Preparation of Liposomes

Compositions of CL and EL containing CA and the CA-HP-β-CD complex are presented in Table 1. Briefly, lipids (5% w/v) and CA (0.15% w/v) were dissolved in required amounts in a chloroform-methanol mixture (13 : 2, v/v) in a round-bottom flask. The solvent was removed by a rotary evaporator (Buchi, Switzerland), leaving a lipid film. The film was hydrated using 8 mL of the phosphate buffer solution (PB, pH 7.4), and the resulting suspension was homogenized using a probe sonicator (Branson, Paramount, CA, USA) at 30% power for 10 min to obtain liposomes in the nanometer-sized range. Non-encapsulated CA was separated by centrifugation immediately after liposome preparation at 17,000 rpm (2236R, Gyrozen Co., Ltd., Korea) to obtain the CA loaded liposomes. The CA remaining in the supernatant was removed and the liposome pellet was resuspended in the PB buffer.

Liposomes containing the CA-HP-β-CD complex, which comprised 0.15% CA, were prepared by the same method except for the hydration step. They were hydrated using 8 mL of the phosphate buffer solution (PB, pH 7.4) containing the CA-HP-β-CD complex (0.15% CA, w/v).

Table 1. Composition of different types of liposomes containing CA and the CA-HP-β-CD complex

Formulations	Egg PC (w/v %)	Cholesterol (w/v %)	Tego® care 450 (w/v %)	CA[a] (w/v %)	CA-HP-β-CD[b] (w/v %)
CL	85	15	-	0.15	-
EL	85	-	15	0.15	-
CD-CL	85	15	-	-	0.15
CD-EL	85	-	15	-	0.15

CL: Conventional liposomes, EL: Elastic liposomes, CD-CL: Conventional liposomes with HP-β-CD, CD-EL: Elastic liposomes with HP-β-CD, CA[a]: Caffeic acid, CA-HP-β-CD[b]: Complex of amount equivalent to 0.15% CA

2-4. Characterization of Liposomes

2-4-1. Particle Size and Zeta Potential Measurement

The particle size and distribution of liposomes were determined by DLS (Otsuka ELS-Z2, Otsuka Electronics, Chiba, Japan) at 25 °C, with a scattering angle of 165, with an Argon laser. The average particle size is indicated by cumulative analysis, and distribution is resolved using the Contin method. The zeta potentials of the liposomes were measured based on electrophoretic mobility under an electric field (Zetasizer, Malvern Instruments, UK).

2-4-2. Deformability Measurement

The deformability of the prepared liposomes was measured with a mini extruder (Avanti polar lipids) and syringe pump (KDS330 Revodix, Korea) as reported [26]. The liposomal suspension (1 mL) was extruded through 0.08 μm size polycarbonate membrane filter for 1 min under pressure of 0.2 MPa. The deformability of the liposomes was calculated as the following equation:

$$\text{Deformability index} = J_{flux} \times (r_v / r_p)^2 \quad (1)$$

where Deformability index represents the deformability value of the vesicles; J_{flux} is the amount of liposomes passed in 3 min; r_v is liposomes size after extrusion; and r_p is pore size of membrane.

2-4-3. Liposome Entrapment Efficiency

Drug entrapment efficiency (EE%) inside the liposomes was determined by the centrifugation technique, which works in principle by determining the amount of non-entrapped drug from the liposomes [27]. The liposomal suspension was centrifuged at 17,000 rpm to obtain the liposome pellet. The supernatant was analyzed by HPLC to determine the amount of non-entrapped CA.

Liposome EE% was calculated according to the following formula:

$$EE\% = (CA_T - CA_F)/CA_T \times 100 \quad (2)$$

CA_T: initially added amount of CA

CA_F: amount of free CA detected in the supernatant after centrifugation

2-4-4. Surface Morphology of Liposomes

Transmission electron microscopy (TEM) analysis was performed for the morphological observation of liposomes using a JEOL-JEM1010 instrument (JEOL Ltd., Tokyo, Japan). Samples were dropped into a carbon-coated copper grid and dried for 2 min. Excess sample was removed using filter paper. Then, the samples were instantly stained with 1% (w/v) phosphotungstic acid allowed to stand for 1 min, and drained. The analysis was performed at an accelerating voltage of 80 kV.

2-4-5. Stability of Liposomes

The prepared liposomes were stored at 4 °C for one month protected from light and macroscopically observed to ensure their integrity. The physical stability of liposomes was evaluated by measuring their particle size and polydispersity index (PDI) at one day and one month after the preparation.

2-5. *In Vitro* Drug Release Studies

The *in vitro* release study was performed using the dialysis membrane method. Prior to use, the dialysis membrane (molecular weight cut-off approximately 12,000-14,000, Sigma, USA) was pretreated by washing the tubing in running water for 4 h to remove the glycerol. Then, sulfur was removed by treatment with a 0.3% (w/v) solution of sodium sulfide at 80 °C for 1 min, followed by acidification with a 0.2% (w/v) sulfuric acid solution. Finally, it was rinsed with water to remove the excess acid. Then, 3 ml of different formulations was placed in the dialysis bag and incubated in 100 mL of release media (phosphate buffer (pH 7.4) with 30% EtOH) at 100 rpm. Then, 1 mL of the release media was collected at appropriate intervals and replaced with equal amount of fresh media. The released CA was quantified by HPLC at 325 nm.

2-6. *In Vitro* Skin Permeation Studies

The *in vitro* skin permeation study with different formulations was carried out using Franz diffusion cells (Permegear, USA). Full-thickness skin was removed from the dorsal side of hairless mice (7 weeks, female). Subcutaneous fat and excess tissue were carefully removed using scalpel and surgical scissors. 5 mL of the receptor phase (EtOH : PBS=3 : 7 (v/v%)) was filled in the receptor chamber and stirred at 150 rpm for 24 h. The skin samples were fixed between the donor and the receptor phase, with the SC layer side facing the donor compartment. The samples (0.4 mL) were applied to the skin in the donor compartment. The skin area contacting the receptor phase was 0.6362 cm^2, and the receptor medium was adjusted at 37 °C to keep temperature of the skin surface at 32 °C. Receptor phase solution (0.4 mL) from each cell was withdrawn through the sampling port at 2, 4, 8, 12, 16, 20 and 24 h. The receptor phase was immediately replaced by equal volume of fresh receptor phase. The withdrawn sample was analyzed by HPLC. The amount of CA retained in skin was determined at the end of the *in vitro* permeation experiment (24 h). The skin surface was washed with PBS solution on each side to remove the rest of samples. The SC was then subsequently removed using the tape-stripping method three times with 3M scotch tape (Korea 3M), and stripped skin was determined by cutting skin into small pieces. The tape and stripped skin were dissolved in 100% ethanol using a sonicator. The concentrations of extracted CA were determined by HPLC.

2-7. HPLC Analysis

The amount of CA was determined using a reversed-phase HPLC system (Shimadzu model, Kyoto, Japan) equipped with an auto-sampler (SIL-20A, Shimadzu), photodiode array detector (SPD-20A, Shimadzu), binary pump (LC-20AT, Shimadzu), column oven (CTO-20A, Shimadzu), and vacuum degasser (DGU-20A, Shimadzu). Chromatographic separation was performed using a Shimpack VP-ODS C_{18} column (4.6×250 mm, 5 μm; Shimadzu, Kyoto, Japan). For HPLC analysis, we used two different linear solvent gradients with a binary mobile phase consisting of 2 v/v% acetic acid in distilled water (solvent A) and 100% acetonitrile (solvent B). The flow rate was set at 1.0 ml/min and the sample injection volume was 20 μl. The column oven temperature was set to 40 °CC and the absorbance was monitored by a UV detector at 325 nm. The amount of CA in formulations was determined with a standard calibration curve for CA obtained in the chromatographic conditions described above.

2-8. Statistical Analysis

All reported data are presented as mean values±standard deviation (SD) of at least three experiments. Statistical significance was determined by one-way analysis of variance (ANOVA) at the level of significance of ($p<0.05$).

RESULTS AND DISCUSSION

1. Characterization of the CA-HP-β-CD Complex

The CA-HP-β-CD complex was prepared by using the freeze-drying method [25]. The CA-HP-β-CD complex appeared as white, amorphous powder, unlike original yellow CA powder. Zhang et al. investigated structural features of the CA-HP-β-CD complex formation by NMR analysis and confirmed that the phenyl ring of the CA is included in the HP-β-CD cavity, while the more polar carboxyl group is exposed outside the HP-β-CD cavity [24]. Therefore, in this study, we did SEM and XRD analyses to confirm the formation of the complex.

SEM micrographs of CA, HP-β-CD, a physical mixture of CA and HP-β-CD, and the CA-HP-β-CD complex are shown in Fig. 1. CA formed irregular shaped crystals (Fig. 1(a)), while HP-β-CD appeared as amorphous spherical particles with cavities (Fig. 1(b)). In a physical mixture of CA and HP-β-CD, both the characteristic crystals of CA and amorphous spheres of HP-β-CD were found (Fig. 1(c)). In contrast, the CA-HP-β-CD inclusion complex appeared as irregular particles with dendrite-like shapes at their ends and the morphology of both original components disappeared (Fig. 1(d)). We concluded that drastic changes in the particle shape indicated that the inclusion complex had been formed by an apparent interaction between CA and HP-β-CD [28].

XRD is a useful method to confirm CD complexation in powder or microcrystalline states. We expected that formation of the inclusion complex between CA and HP-β-CD would lead to the loss of CA crystalline characteristics. In addition, the diffraction pattern of the complex had to be qualitatively different from a mere superposition of the original components [29]. XRD patterns of CA, HP-β-CD, a physical mixture of CA and HP-β-CD, and the CA-HP-β-CD complex are shown in Fig. 2. CA XRD pattern showed intense, sharp peaks in the crystalline form (Fig. 2(a)), while HP-β-CD manifested an amorphous structure that lacked crystalline peaks (Fig. 2(b)). The XRD pattern of the physical mixture of CA and HP-β-CD represented a superposition of the crystalline CA pattern and amorphous HP-β-CD pattern, confirming that no inclusion was formed (Fig. 2(c)). In contrast, the inclusion complex was characterized by an amorphous pattern, similar to that of HP-β-CD, while the characteristic diffraction peaks of CA were completely absent (Fig. 2(d)). These results confirmed that CA had been incorporated within the HP-β-CD matrix with the formation of the CA-HP-β-CD inclusion complex.

2. Characterization of Liposomes

2-1. Particle Size and Zeta Potential of Liposomes

We prepared liposomes that contained CA and the CA-HP-β-CD complex and compared their physicochemical characteristics. The particle size, PDI, and zeta potential of these liposomes are

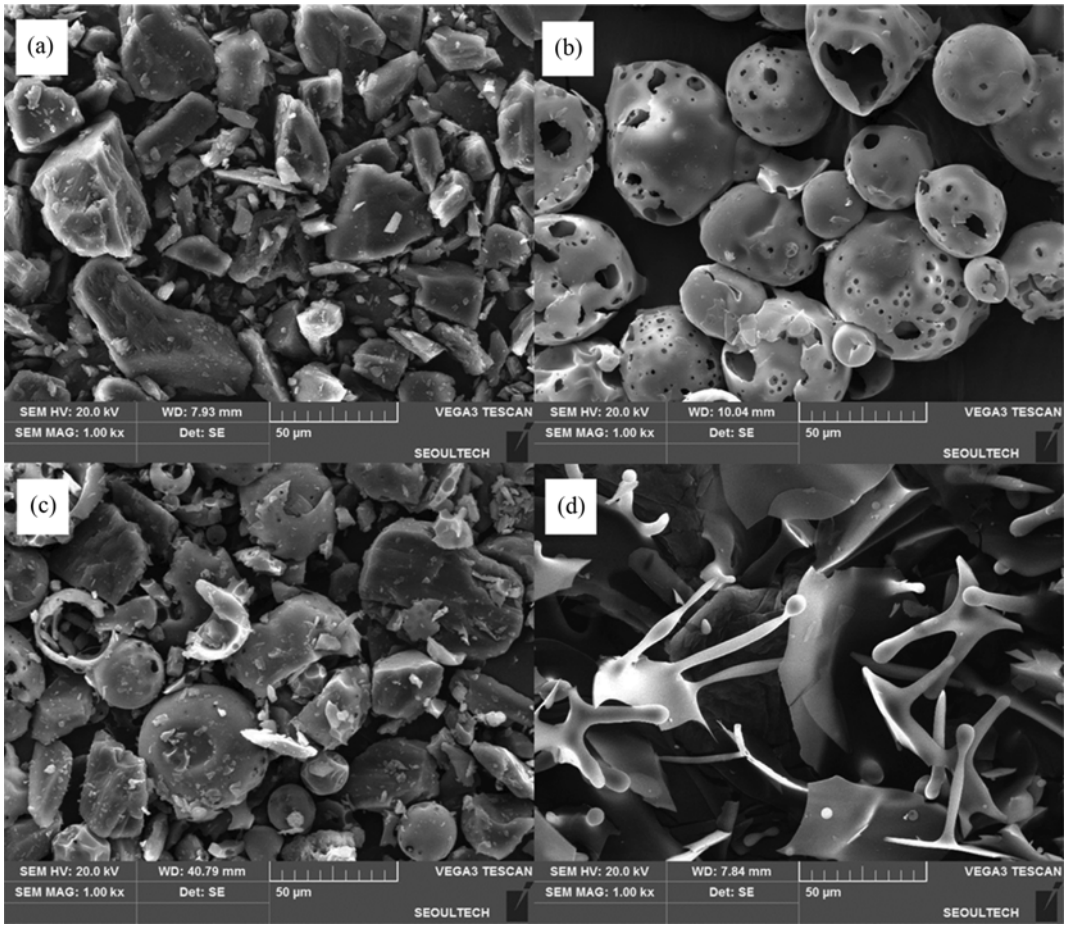

Fig. 1. SEM micrographs of CA (a), HP-β-CD (b), a physical mixture of CA and HP-β-CD (c), and the CA-HP-β-CD complex (d).

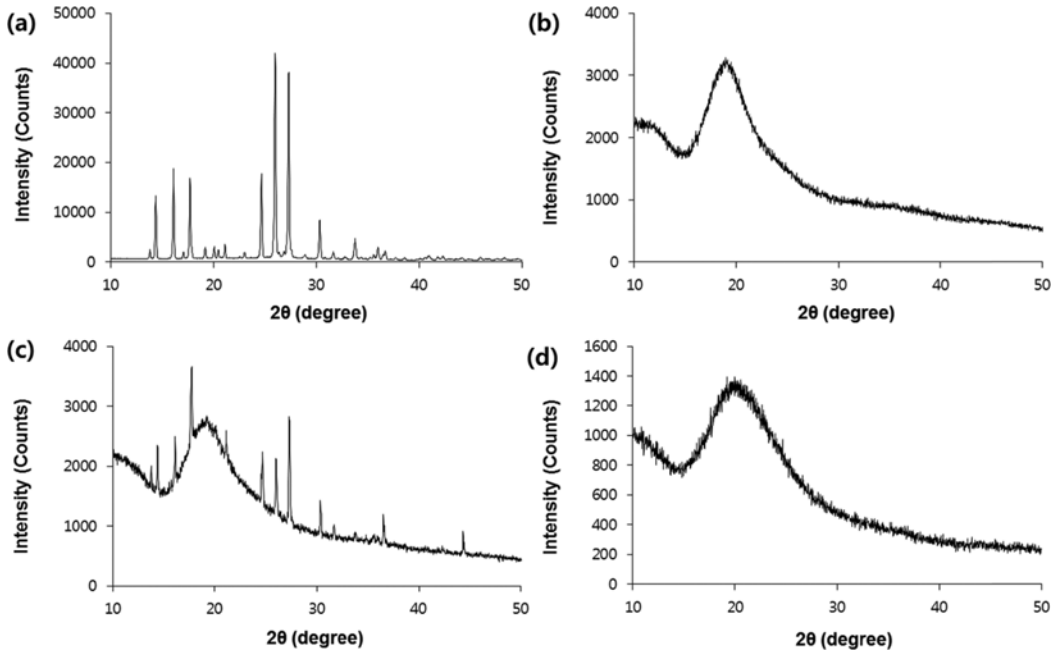

Fig. 2. Powder X-ray diffraction patterns of CA (a), HP-β-CD (b), a physical mixture of CA and HP-β-CD (c), and the CA-HP-β-CD complex (d).

Table 2. Mean particle size, polydispersity index, zeta potential, and deformability index of liposome preparations containing CA and the CA-HP-β-CD complex (mean±SD, n=3)

Codes	Particle size (nm)	PDI	Zeta potential (mv)	Deformability index
CL	198.8±0.8	0.17±0.02	−27.8±2.2	8.88±0.32
EL	147.6±0.9	0.22±0.01	−35.9±1.6	13.79±0.64
CD-CL	191.2±1.9	0.16±0.01	−37.9±3.2	10.10±0.38
CD-EL	138.8±4.1	0.24±0.01	−37.0±2.2	14.61±0.69

listed in Table 2. As controls, the particle size values were 190.3, 135.9, 181.0 and 130.7 nm for CL, EL, CD-CL and CD-EL without CA, respectively (data not shown). The particle size of elastic liposomes (EL and CD-EL) was lower than that of conventional liposomes (CL and CD-CL). This could be due to increased flexibility and decreased surface tension of elastic vesicles caused by the use of Tego® care 450 as an edge activator [30]. Moreover, liposomes containing the CA-HP-β-CD complex (CD-CL and CD-EL) tended to have a smaller size than liposomes without HP-β-CD (CL and EL). This phenomenon could also be caused by a decrease of surface tension due to the addition of HP-β-CD. In addition, a reduction of entropy of liposomes by CDs may have stabilized the small vesicles, as observed by Alomrani et al. [31]. PDI values were in the range of 0-0.3, which indicated a homogeneous dispersion.

Zeta potential is the electrostatic potential on the liposome surface, which affects vesicular properties, physical stability, and skin-vesicle interactions. High liposome zeta potential prevented aggregation of liposomes and increased their stability [32]. All liposomes that included CA had a negative electric charge of approximately −30 mV. This was because the carboxylic group of CA and OH groups of the sugar moiety in Tego® care 450 are negatively charged in the buffer solution at pH 7.4 [24,33]. Such a high absolute value of the zeta potential stabilized liposomes because particle aggregation was prevented by a high level of mutual repulsion.

2-2. Deformability of Liposomes

Membrane deformability is an important property that differentiates EL from CL. Deformable membranes help vesicles to deliver active compounds deeply into the skin by facilitating penetration through the skin pores that are much smaller than the vesicle diameter [34]. Deformability of prepared liposomes was investigated by the extrusion method (Table 2). Deformability indices of CL and CD-CL were 8.88 and 10.10, respectively. Higher deformability indices were determined for EL and CD-EL, which contained an edge activator (13.79 and 14.61, respectively). We concluded that presence of an edge activator in liposomes disrupted packing characteristics of phospholipids in the liposome bilayer, which led to increased membrane deformability [35].

2-3. CA Entrapment Efficiency

We measured CA EE% in liposomes containing CA and the CA-HP-β-CD complex (Fig. 3). EE% values in CL and EL comprised 42.58% and 47.04%, respectively. Higher EE% values, 68.17% and 73.25%, were observed in CD-CL and CD-EL with HP-β-CD, respectively, which was approximately 1.6-fold higher than EE% in CL and EL. In the latter case, enhanced EE% could be attributed to a well-known solubilizing ability of HP-β-CD. It was reported that CD complexation enhances drug solubilization and entrapment in the aqueous liposome core [36]. In this way, larger quantities of CA in the form of CA-HP-β-CD complexes could be encapsulated into the aqueous liposomal core within a volume relatively larger than that of lipid bilayers [37].

2-4. Morphology of Liposomes

Fig. 4 shows TEM images of structural morphology of different liposome preparations. All liposomes maintained their spherical

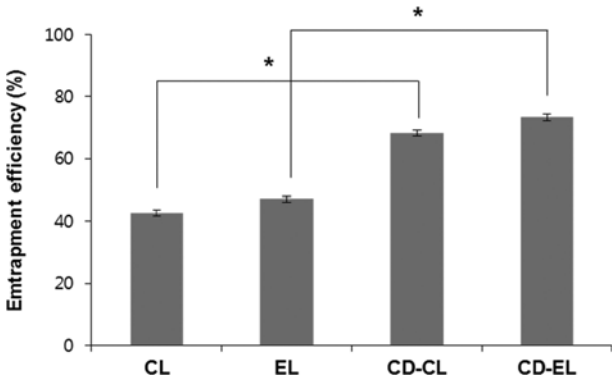

Fig. 3. Entrapment efficiency of different liposomal preparations that contained CA and the CA-HP-β-CD complex (mean± SD, n=4).

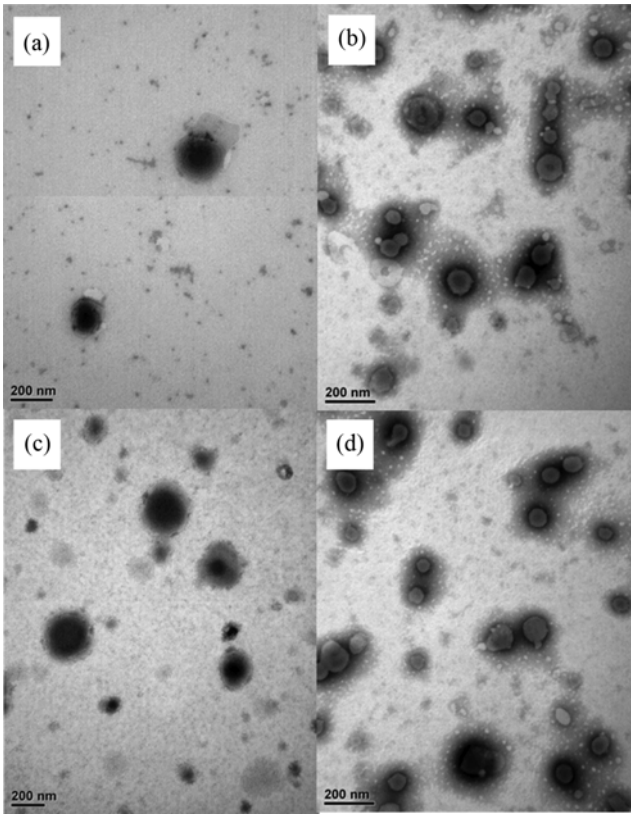

Fig. 4. Transmission electron microscopy images of different liposomes containing CA and the CA-HP-β-CD complex; (a) CL, (b) EL, (c) CD-CL and (d) CD-EL.

shape and vesicular structure and appeared to be homogenously small. Fig. 4(b), (d) demonstrates that liposome morphology was retained after the incorporation into the CD complex. This indicates that entrapment of the drug-CD inclusion complex within the liposome did not affect bilayer structure and lamellar integrity [38].

2-5. Stability of Liposomes

Changes of particle size and PDI value are important indicators of the physical stability of the liposome membrane. To investigate

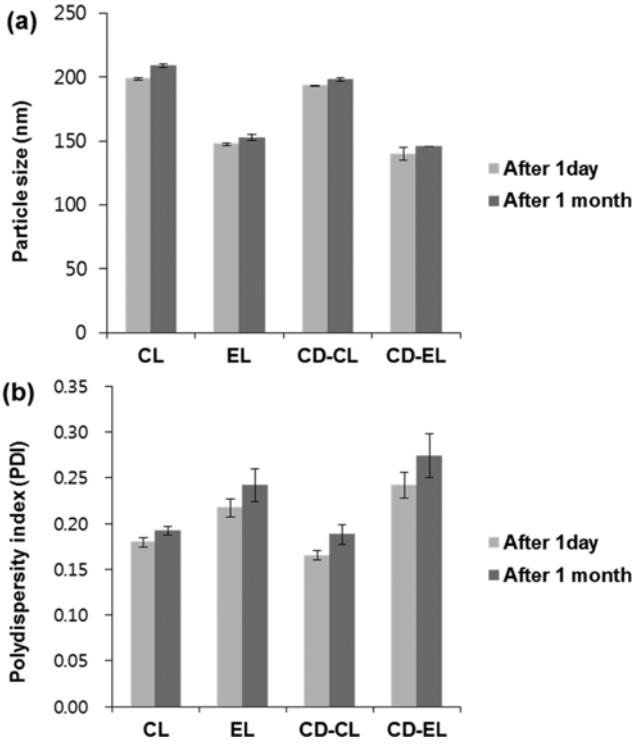

Fig. 5. Storage stability of liposomes containing CA and the CA-HP-β-CD complex: (a) change of particle size distribution, (b) change of polydispersity index (PDI) over 1 month. Values are presented as mean±SD (n=3).

liposome stability, we visually inspected liposome preparations and measured the change in their particle size and PDI at 4 °C after 1 month of storage at 4 °C (Fig. 5). Particle sizes of different populations of liposomes were stable and did not differ significantly from their initial values after one month of storage. PDI values remained under 0.3. In addition, phase separation and flocculation were not observed; therefore, we confirmed that prepared liposomes were stable for at least one month.

3. *In Vitro* Drug Release Studies

The diffusion of an entrapped molecule from a vesicular system is governed by its transfer from the delivery system into the external aqueous phase and diffusion through the dialysis membrane into the external compartment. Only the molecules present in the external aqueous phase are able to permeate through the membrane [39]. *In vitro* drug release profiles of different formulations are shown in Fig. 6. The release profiles of CL, EL, CD-CL, and CD-EL were compared to those of the CA solution and CA-HP-β-CD complex solution dissolved in PB buffer as control formulation. To facilitate dissolution of CA, we added 20% 1,3-BG to the CA solution. 1,3-BG is widely used as an ingredient for dissolving active components in cosmetics and has skin moisturizing properties. The release rate of different formulations increased in the following order: CA solution>CA-HP-β-CD complex solution>EL>CL>CD-EL>CD-CL. As shown in Fig. 6, the CA solution, as a control formulation, exhibited a rapid drug release behavior with 97.8% of CA being released after 4 h. This mode of release suggested that there was no interaction of the drug with the dialysis

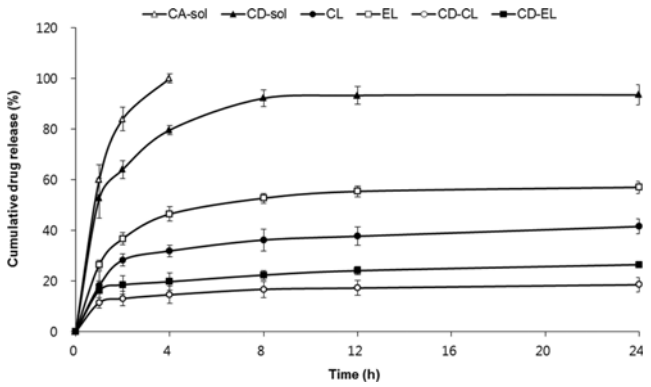

Fig. 6. *In vitro* drug release profiles of different formulations containing CA and the CA-HP-β-CD complex. Values are expressed as the mean±SD (n=3).

membrane under our experimental conditions [40]. The release of CA from the CA-HP-β-CD complex solution was slower with 79.6% and 93.6% being released after 4 and 24 h, respectively. The slower release of the drug from the CA-CD complex solution in comparison to the release rate from the CA solution could be due to the formation of the complex. On the other hand, entrapment of CA into liposomal vesicles allowed a better control over the drug release rate compared to its rapid liberation from solutions.

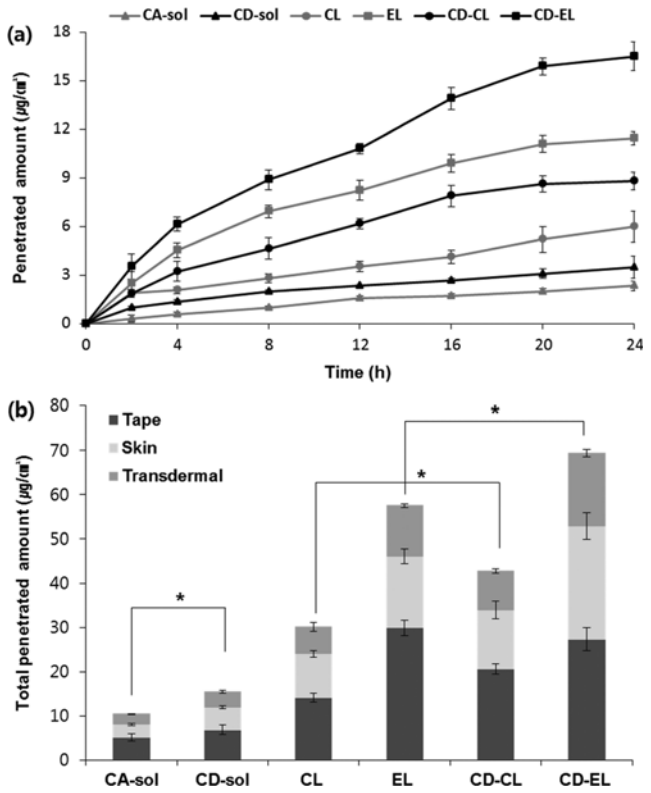

Fig. 7. (a) *In vitro* skin permeation profiles, (b) total permeation amount of CA from the different formulations into the skin of hairless mice after 24 h (Tape: stratum corneum, Skin: epidermis and dermis without stratum corneum, Transdermal: receptor phase). *p<0.05.

This difference was probably due to the well-known reservoir effect of liposomes [27]. After 24 h, 41.5% and 57.1% of CA was released from CL and EL, whereas only 18.5% and 26.5% CA was released from CD-CL and CD-EL, respectively. Liposomes with HP-β-CD showed relatively slow and sustained release profiles. This behavior can be explained by the formation of an additional barrier to the release of the drug from the vesicle membranes because of complexation. In addition, slower release could occur due to the stabilization of the vesicle membrane by CD [41,42]. Thus, our study confirmed the utility of CD for controlled and sustained drug release.

4. *In Vitro* Skin Permeation Studies

In vitro skin permeation profiles of different CA-loaded formulations were obtained using Franz diffusion cells (Fig. 7). We used 0.15% CA solution with 20% 1,3-BG and CA-HP-β-CD complex solution as control groups. All formulations were applied to the skin surface under occlusive conditions for 24 h. The amount of CA in the receptor phase that had permeated through the skin in a constant area (0.6362 cm^2) during 24 h is shown in Fig. 7(a). Transdermal CA penetration across the skin showed a time-dependent increase for all formulations. After 24 h, liposomal vesicles mediated relatively higher levels of cumulative CA permeation than did the CA solution and CA-CD complex solution. Among liposomal vesicles, CD-EL (16.52 μg/cm^2) allowed for the highest permeation levels, followed by EL (11.46 μg/cm^2). Although conventional liposomes, such as CL and CD-CL, provided lower permeation levels (6.05 μg/cm^2 and 8.82 μg/cm^2, respectively) than elastic liposomes, there were still significantly more effective than the CA solution (2.34 μg/cm^2) and CA-CD complex solution (3.49 μg/cm^2). Thus, transdermal skin permeation studies indicated that our DCEL system, which combined CDs and elastic liposomes, enhanced transdermal delivery of CA. We believe that the small size of the obtained particles and high deformability of EL positively affected CA permeation. Furthermore, it was reported that CDs enhance percutaneous absorption of drugs due to their solubilizing action, which increases drug availability at the absorption site [43]. CDs also facilitate interactions with free lipids present in the SC layer and thereby potentiate transdermal permeation of drugs [44]. Fig. 7(b) shows the total permeation amount of CA present in the stratum corneum (Tape), in the epidermis and dermis except for stratum corneum (Skin) and in receptor phase passing through skin (Transdermal) by quantitative analysis. The total skin permeation of CA-HP-β-CD loaded liposomes was significantly higher than that obtained for CA alone. Thus, the total skin permeation amount of CD-CL (42.76 μg/cm^2) was 1.4-fold higher than that of CL (30.09 μg/cm^2). The same parameter in CD-EL (69.40 μg/cm^2) was 1.2-fold higher than that of EL (57.54 μg/cm^2). Of all preparations, CD-EL provided the highest total skin permeation amount, which was 6.7-fold higher than the amount determined in the experiment with the control CA solution (10.30 μg/cm^2). The relatively higher level of skin permeation observed when using CD-EL could be attributed to the synergistic effect of CD complexation and elastic liposomes. Elastic liposomes are able to increase skin permeation due to the high degree of their deformability, which modifies the intercellular lipid lamellae and facilitates fusion of vesicles with the skin [45]. CDs have been reported previously to act as skin penetration enhancers. In an SEM study, Singh et al. demonstrated that CD in-

creases permeation of drugs by inducing intercellular lipid perturbations with pore formation on the skin surface [41]. Furthermore, the increase in solubility, higher entrapment efficiency, and sustained drug release of HP-β-CD could have contributed to enhanced permeation of CA through the skin [17]. Therefore, this study suggests that our DCEL system that combined CDs and elastic liposomes can considerably enhance skin permeation of drugs.

CONCLUSION

We prepared a DCEL system that combines advantages of drug-CD complexes and elastic liposomes to enhance skin permeation of CA. The prepared DCEL system was compared and evaluated with different liposomal preparations (CL, EL, and CD-CL). The presence of Tego® care 450 reduced the vesicle size and increased membrane deformability of elastic liposomes. The entrapment efficiency of liposomes was enhanced by the addition of HP-β-CD. *In vitro* release studies demonstrated that CD-EL provided more sustained CA release profiles than those obtained with the free CA solution. Similarly, the permeation ability of CD-EL was greater than that of other liposomal preparations. Such enhancement could be due to the small particle size, high deformability, and increased entrapment efficiency of CD-EL. Therefore, the results of this study suggest that elastic liposomes containing the HP-β-CD complex (DCEL system) have a potential to become a promising transdermal delivery system for the delivery of pharmacologically active compounds including CA.

ACKOWLEDGEMENTS

This work was conducted with the support of the Cooperative Research Program for Agriculture Science & Technology Development (Project No. 008489) Rural Development Administration, Republic of Korea.

REFERENCES

1. P. L. Honeywell-Nguyen and J. A. Bouwstra, *Drug Discovery Today Technol.*, **2**, 67 (2005).
2. D. P. Otto and M. M. Villiers, *Ther. Deliv.*, **5**, 961 (2014).
3. S. N. Park, M. H. Lee, S. J. Kim and E. R. Yu, *Biochem. Biophys. Res. Commun.*, **435**, 361 (2013).
4. M. J. Choi and H. I. Maibach, *Int. J. Cosmet. Sci.*, **27**, 211 (2005).
5. G. Cevc and G. Blume, *BBA-Biomembranes*, **1104**, 226 (1992).
6. M. A. Elsayed, Y. Abdallah, F. Naggar and M. Khalafallah, *Int. J. Pharm.*, **332**, 1 (2007).
7. W. Johnson, *Int. J. Toxicol.*, **20**, 13 (2001).
8. S. B. Han, S. S. Kwon, Y. M. Jeong, B. J. Kong, E. R. Yu and S. N. Park, *Polymer (Korea)*, **38**, 694 (2014).
9. S. N. Park, M. S. Lim, M. A. Park, S. S. Kwon and S. B. Han, *Polymer (Korea)*, **36**, 705 (2012).
10. F. Maestrlli, M. L. González-Rodríguez, A. M. Rabasco, C. Ghelardini and P. Mura, *Int. J. Pharm.*, **395**, 222 (2010).
11. N. R. Im, H. S. Kim, K. J. Kim, G. Y. Noh and S. N. Park, *Appl. Chem. Eng.*, **26**, 563 (2015).
12. W. Zhang, G. Wang, J. R. Falconer, B. C. Baguley, J. P. Shaw, J. Liu, H. Xu, E. See, J. Sun, J. Aa and Z. Wu, *Pharm. Res.*, **32**, 1451 (2015).
13. B. McCormack and G. Gregoriadis, *Int. J. Pharm.*, **112**, 249 (1994).
14. J. Chen, W. L. Lu, W. Gu, S. S. Lu, Z. P. Chen, B. C. Cai and X. X. Yang, *Expert. Opin Drug. Deliv.*, **11**, 565 (2014).
15. J. Chen, W. L. Lu, W. Gu, S. S. Lu, Z. P. Chen and B. C. Cai, *Expert. Opin Drug. Deliv.*, **10**, 845 (2013).
16. K. Cal and K. Centkowska, *Eur. J. Pharm. Biopharm.*, **68**, 467 (2008).
17. N. Kaur, R. Puri and S. K. Jain, *Aaps PharmSciTech*, **11**, 528 (2010).
18. T. Loftsson and M. E. Brewster, *J. Pharm. Pharmacol.*, **63**, 1119 (2011).
19. N. J. Kang, K. W. Lee, B. J. Shin, S. K. Jung, M. K. Hwang, A. M. Bode, Y. S. Heo, H. J. Lee and Z. Dong, *Carcinogenesis*, **30**, 321 (2009).
20. A. Gupta, D. K. Maheshwari and G. Khandelwal, *J. Appl. Nat. Sci.*, **5**, 459 (2013).
21. T. A. Astorino and K. A. Alkadhi, in *Caffeine: chemistry, analysis, function and effects*, V. R. Preedy Eds., Royal Society of Chemistry (2012).
22. B. Y. Kim, J. S. Jeong, H. J. Kwon, J. H. Lee and S. P. Hong, *Kor. J. Herbol.*, **23**, 67 (2008).
23. M. Fathi, M. Mirlohi, J. Varshosaz and G. Madani, *J. Nanomater.*, **2013**, 9 (2013).
24. M. Zhang, J. Li, L. Zhang and J. Chao, *Spectrochim. Acta, Part A.*, **71**, 1891 (2009).
25. P. R. K. Mohan, G. Sreelakshmi, C. V. Muraleedharan and R. Joseph, *Vib. Spectrosc.*, **62**, 77 (2012).
26. B. A. I. van den Bergh, P. W. Wertz, H. E. Junginger, J. A. Bouwstra, *Int. J. Pharm.*, **217**, 13 (2001).
27. J. Shaji and S. Iyer, *Asian J. Pharm.*, **6**, 218 (2012).
28. A. Delrivo, A. Zoppi and M. R. Longhi, *Carbohydr. Polym.*, **87**, 1980 (2012).
29. B. Liu, J. Zhao, Y. Liu, X, Zhu and J. Zeng, *J. Agric. Food Chem.*, **60**, 12501 (2012).
30. A. Gillet, F. Lecomte, P. Hubert, E. Ducat, B. Evrard and G. Piel, *Eur. J. Pharm. Biopharm.*, **79**, 43 (2011).
31. A. H. Alomrani, G. A. Shazly, A. A. Amara and M. M. Badran, *Colloids Surf., B.*, **121**, 74 (2014).
32. F. Guo, J. Wang, M. Ma, F. Tan and N. Li, *J. Mater. Sci. Mater. Med.*, **26**, 1 (2015).
33. A. Hommoss, PhD Thesis, Berlin, Free University of Berlin (2009).
34. N. Aggarwal and S. Goindi, *Int. J. Pharm.*, **437**, 277 (2012).
35. G. M. M. El Maghraby, A. C. Williams and B. W. Barry, *Int. J. Pharm.*, **276**, 143 (2004).
36. S. S. Dhule, P. Penfornis, T. Frazier, R. Walker, J. Feldman, G. Tan, J. He, A. Alb, V. John and R. Pochampally, *Nanomedicine*, **8**, 440 (2012).
37. H. Agashe, P. Lagisetty, K. Sahoo, D. Bourne, B. Grady and V. Awasthi, *J. Nanopart. Res.*, **13**, 2609 (2011).
38. J. Shaji and M. Lal, *Int. J. Curr. Pharm. Res.*, **6**, 16 (2014).
39. G. Nava, E. Pinon, L. Mendoza, N. Mendoza, D. Quintanar and A. Ganem, *Pharmaceutics*, **3**, 954 (2011).
40. A. Hussain, A. Samad, M. Ramzan, M. N. Ahsan, Z. Ur Rehman and F. J. Ahmad, *Drug. Deliv.*, **14**, 1 (2014).
41. H. P. Singh, A. K. Tiwary and S. Jain, *Yakugaku Zasshi*, **130**, 397, (2010).
42. M. C. Lira, M. S. Ferraz, D. G. da Silva, M. E. Cortes, K. I. Teixeira,

N. P. Caetano and N. S. Santos-Magalhães, *J. Incl. Phenom. Macrocycl. Chem.*, **64**, 215 (2009).
43. M. Masson, T. Loftsson, G. Masson and E. Stefansson, *J. Control. Release*, **59**, 107 (1999).
44. M. S. Nagarsenker, L. Amin and A. A. Date, *AAPS PharmSciTech*, **9**, 1165 (2008).
45. D. Chirio, R. Cavalli, F. Trotta, M. E. Carlotti and M. Trotta, *J. Incl. Phenom. Macrocycl. Chem.*, **57**, 645 (2007).